BARC/2009/E/005

GAMMA RAY SELF-ATTENUATION CORRECTION: A SIMPLE NUMERICAL APPROACH AND ITS VALIDATION

by

Chhavi Agarwal, Sanhita Poi, Amol Mhatre and A. Goswami
Radiochemistry Division

2009

BARC/2009/E/005

BARC/2009/E/005

GOVERNMENT OF INDIA
ATOMIC ENERGY COMMISSION

GAMMA RAY SELF-ATTENUATION CORRECTION: A SIMPLE NUMERICAL APPROACH AND ITS VALIDATION

by

Chhavi Agarwal, Sanhita Poi, Amol Mhatre and A. Goswami
Radiochemistry Division

BHABHA ATOMIC RESEARCH CENTRE
MUMBAI, INDIA
2009

BIBLIOGRAPHIC DESCRIPTION SHEET FOR TECHNICAL REPORT
(as per IS : 9400 - 1980)

01	*Security classification :*	Unclassified
02	*Distribution :*	External
03	*Report status :*	New
04	*Series :*	BARC External
05	*Report type :*	Technical Report
06	*Report No. :*	BARC/2009/E/005
07	*Part No. or Volume No. :*	
08	*Contract No. :*	
10	*Title and subtitle :*	Gamma ray self-attenuation correction: a simple numerical approach and its validation
11	*Collation :*	51 p., 13 figs., 3 tabs., 1 ill.
13	*Project No. :*	
20	*Personal author(s) :*	Chhavi Agarwal; Sanhita Poi; Amol Mhatre; A. Goswami
21	*Affiliation of author(s) :*	Radiochemistry Division, Bhabha Atomic Research Centre, Mumbai
22	Corporate author(s) :	Bhabha Atomic Research Centre, Mumbai-400 085
23	*Originating unit :*	Radiochemistry Division, BARC, Mumbai
24	*Sponsor(s) Name :* *Type :*	Department of Atomic Energy Government

Contd...

30	*Date of submission :*	February 2009
31	*Publication/Issue date :*	March 2009
40	*Publisher/Distributor :*	Associate Director, Knowledge Management Group and Head, Scientific Information Resource Division, Bhabha Atomic Research Centre, Mumbai
42	*Form of distribution :*	Hard copy
50	*Language of text :*	English
51	*Language of summary :*	English, Hindi
52	*No. of references :*	9 refs.
53	*Gives data on :*	
60	*Abstract :* A hybrid Monte Carlo method for gamma ray attenuation correction has been developed. The method has been applied to some common counting geometries like cylinder, box, sphere and disc. The method has been validated theoretically and experimentally over a wide range of transmittance and sample-to-detector distances. The advantage of the approach is that it is common to all sample geometries and can be used at all sample-to detector distances.	
70	*Keywords/Descriptors :*	GAMMA RADIATION; VALIDATION; M CODES; GAMMA SPECTROSCOPY; MONTE CARLO METHOD; YTTERBIUM 169; URANIUM 235
71	*INIS Subject Category :*	S38
99	*Supplementary elements :*	

गामा किरण तनुकरण शोधन हेतु एक हाइब्रिड मांटे कार्लों पद्धति विकसित की गई है । इस पद्धति का अनुप्रयोग बेलनाकार, चौकोर, बॉक्स, गोल एवं चक्रिका जैसी सामान्य ज्यामितियों की गणना के लिए किया गया । पद्धति को संचार एवं सैंपल से संसूचक की दूरियों के व्यापक परास हेतु सैद्धांतिक एवं अनुप्रयोगात्मक रूप से मान्यकृत किया गया । इसका यही लाभ है कि यह सभी सैंपल ज्यामितियों में समान है तथा सभी वस्तु से संसूचक(सैंपल टू डिटेक्टर) तक की दूरियों में भी प्रयोग में लायी जा सकती है ।

कुंजीशब्द : स्व-तनुकरण; सांख्यिक पद्धति; मांटे कार्लो; दूर क्षेत्र ज्यामिति; निकट क्षेत्र ज्यामिति

Abstract

A hybrid Monte Carlo method for gamma ray attenuation correction has been developed. The method has been applied to some common counting geometries like cylinder, box, sphere and disc. The method has been validated theoretically and experimentally over a wide range of transmittance and sample-to-detector distances. The advantage of the approach is that it is common to all sample geometries and can be used at all sample-to detector distances.

Keywords: Self-attenuation; Numerical method; Monte Carlo; Far-field geometry; Near-field geometry.

1. Introduction

Passive non-destructive assay techniques rely on the measurement of gamma radiation emitted spontaneously from nuclear materials. This type of assay often requires measurement of the gamma rays from samples of varied sizes, shapes and also different physical states. Gamma ray emitted from such diverse samples often suffers from scattering or absorption within the sample. This results in the lack of proportionality between the count rate for the gamma ray monitored and the amount of the nuclide emitting the gamma ray. In such cases, the exact knowledge about the sample amount is only possible by accurate correction for gamma ray self attenuation. Use of the standards cannot solve the problem of the gamma ray self attenuation since the chemical composition as well as the shape and size of the sample can vary widely. Determination of attenuation correction factor is therefore very necessary to increase the linear dynamic range of concentration that can be determined by gamma ray spectrometry. This also makes the technique independent of other components present in the sample. A detailed description of attenuation correction for different sample-detector geometries is given in [1]. The corrected count rate *(CR)* of a gamma-emitting radionuclide from a sample of given size and shape is given by:

$$CR = k_{att}\, x\, k_{rate}\, x\, RR \qquad (1)$$

where k_{att} , k_{rate} are the correction factors for attenuation in the sample and for rate-related losses which includes electronic loss as well as summing effect respectively and *RR* is the count rate of the gamma ray of interest registered in the detection system. *CR* can be used to obtain the mass *(M)* of the isotope emitting the gamma ray of interest using the standard equation:

$$CR = K\ x\ M \tag{2}$$

The proportionality constant *(K)* is the disintegration rate per unit mass of the sample which can be obtained using a standard of same shape as that of the sample.

The attenuation correction factor (k_{att}) is the fraction of gamma rays that are absorbed or scattered within the sample and are not able to reach the detector. It is defined as:

$$k_{att} = \frac{RR(\mu_L = 0, specified\ shape)}{RR(\mu_L \neq 0, real\ shape)} \tag{3}$$

where *RR* (μ_L = 0, specified shape) is the count rate for totally non-attenuating (μ_L = 0) sample having a specified shape. This specified shape may not necessarily be the actual shape of the sample and can be approximated to be a simplified shape like a point or a line depending upon the sample-detector configuration. *RR* ($\mu \neq 0$, real shape) is the measured count rate for the sample. The measurement of attenuation correction factor is generally a two step process. First step is the determination of linear attenuation coefficient (μ_L) of the sample. The next step is to choose an appropriate model to obtain the sample-detector geometry dependent attenuation correction factor. The two steps involved are discussed in detail below:

1.1. Measurement of linear attenuation coefficient (μ_L).

The linear attenuation coefficient (μ_L) of the sample can be determined either theoretically by taking the literature mass attenuation coefficient (μ_m) at the monitored energy and correcting it for the density of the sample. This requires the precise knowledge of density and the composition of the sample which may not always be

feasible to measure accurately. The other commonly used method is to measure μ_L experimentally by transmission technique. The experimental set up for this is shown in figure 1. Here, the transmission of a collimated beam of gamma ray from an external source is measured with and without the sample. Then, the linear attenuation coefficient is obtained from the relation**:**

$$I = I_o \exp(-\mu_L x) \tag{4}$$

where, I and I_o are the intensity of gamma ray with and without the sample, x is the distance traversed by the gamma ray through the sample. Here the choice of external source is important and depends upon the radionuclides monitored. In principle, one should use a transmission source that emits a gamma ray of energy as close as possible to the energy of the gamma ray emitted by the sample and should be preferably monoenergetic.

1.2. Calculation of attenuation correction factor *(k_{att}):*

Once the μ_L of the sample is known, one has to use an appropriate model to obtain the sample-detector geometry dependent attenuation correction factor. As it is looking from equation 3, the calculation of attenuation correction factor is not that simple and is generally obtained computationally. The equation in that case can be expressed as:

$$k_{att} = \frac{\int_v \rho I \varepsilon dV}{\int_v \rho I \varepsilon \exp(-\mu_L t) dV} \tag{5}$$

where ρ = spatial density of the isotope being assayed (g/cm^3),

I = emission rate of the assayed gamma ray (γ/g-s),

ε = absolute full energy detection efficiency,

μ_L = linear attenuation coefficient of the sample,

and t = distance the gamma ray travels within the sample.

Here, the factor ρI will remain constant in both numerator and denominator for a homogeneous sample and will cancel out. Since ε is a function of the co-ordinate of the point at which gamma ray originates within the sample, it cannot be taken out of the integral and hence it will not cancel out. If the sample-to-detector distance is quite large compared to the sample dimensions so that the gamma rays reaching the detector are essentially parallel then ε can be assumed to be independent of point of origin of the gamma ray within the sample and can be taken out of integrals, so that the integrals becomes relatively easy to compute. The situation is called far-field case and k_{att} becomes independent of the detector size, shape and sample-to-detector distance and is only influenced by the sample characteristics like its size and shape. For far-field cases, analytical expressions are available in literature for different sample geometries viz. box-shaped (rectangular parallelepiped), cylindrical [2] and spherical [3].

In practice, it is not always possible to count the sample far away from the detector. For example, with environmental samples, activity is usually low, and the sample is required to be counted close to the detector to maximize the count rate. In such a case, the far-field formulae cannot be applied as they neglect the detector geometry and assume detector to be a point detector. In literature, separate numerical models are available for calculating attenuation correction factors for the near-field case. These models are based on simplification of sample-detector geometry. For example, in k_{att} calculation for disc geometry [1] the sample is assumed to be a line sample instead of a disc and the detector

is considered to be a point detector. Also it is assumed that the sample-to-detector distance is few times greater than the detector and sample radius. Similarly, in k_{att} calculation for cylindrical samples in near-field geometry [1], the sample is assumed to be circular in shape and the detector is again assumed to be a point detector. Moreover, there are restrictions about sample-detector dimensions.

A semi-empirical procedure to calculate detector efficiency for a point, disc and cylindrical samples has been described in [4]. The method takes care of gamma ray attenuation within the sample. The peak efficiency of any investigated configuration ($\varepsilon_{p,x}$) is calculated from the measured efficiency of a reference point source ($\varepsilon_{p,ref}$) positioned on the detector axis at large distance from the detector using the formula:

$$\varepsilon_{p,x} = \varepsilon_{p,ref} \frac{\bar{\Omega}_x}{\bar{\Omega}_{ref}} \tag{6}$$

where $\overline{\Omega}_{ref}$ and $\overline{\Omega}_x$ are the effective solid angles of the point source and the sample respectively. $\overline{\Omega}_{ref}$ takes into account the attenuation within the sample. The effective solid angle is related to the peak efficiency (ε_p) as:

$$\varepsilon_p = \frac{1}{4\pi} \frac{P}{T} \overline{\Omega} \tag{7}$$

where *P/T* is peak to total ratio for the detector for the given gamma ray. The method involves numerical integration for the evaluation of $\overline{\Omega}_i$, and requires detector dimensions as input. Debertin et. al. [5] proposed a point detector model for calculation of detector efficiency from attenuating samples. Alternative to all these approaches is a full scale Monte Carlo calculation of k_{att} which is quite time consuming. It also requires a detailed

description of sample-detector geometry and sample composition. Recently, a hybrid Monte Carlo method has been used to calculate detector efficiency [6] and self-attenuation correction factors [7] where analytical expressions are used in Monte Carlo simulation. This leads to considerable reduction in computation time.

2. Motivation behind the present work

From the above discussion, it can be concluded that although there are several approaches available in the literature but none is valid at all sample-detector geometries. Also it is not easy to decide which formula to use as it not only depends upon the sample-to-detector distance but also on the sample-detector dimensions. For eg. a distance of 10 cm may be a far-field for 20 ml vial but not for a 200 L drum. Therefore, inspite of so many approaches available in literature, for laboratories where attenuation correction is a part of routine analysis, a simple, convenient method is still very much required which can be applied without bothering much about sample-detector geometry. In the present report, a hybrid Monte Carlo method to calculate k_{att} has been described for some common counting geometry like spherical, cylindrical and box-shaped samples. This method avoids any simplified assumption used for near or far-field geometry formulae. Moreover, unlike the far-field and near-field approaches, the detector is not considered to be a point detector. This method does not require detailed information about detector dimensions and only the radius of the detector crystal (considered to be a cylinder) comes into picture in the calculations.

3. Present work

In this work, attenuation correction factors for the three geometries i.e. cylinder, sphere and box have been calculated at different sample-to-detector distances as a function of transmittance and these results are compared with the analytical expressions available in the literature. MCNP calculations [8] have also been performed to validate the prediction of our calculation for samples of varied transmittance and sample-to-detector distance. This method has been validated by comparing the results of calculation with the experimentally obtained k_{att}*'s*. The experiment was done at three geometries – 1) cylindrical sample with axis collinear with the detector axis (disc geometry), 2) cylindrical sample with axis perpendicular to detector axis (cylindrical geometry) and 3) box shaped sample. In all the cases, the centre of gravity of the sample was lying on the detector axis. All the three geometrical set-ups are shown in figure 2.

4.1. Hybrid Monte Carlo method

In equation 5, as already emphasized above, all the factors cancels out except ε and the exponential term. As mentioned before, ε is the efficiency of the detector for particular sample-detector geometry and so is inversely proportional to $1/r^2$ where r is the distance the gamma ray travels from the sample to detector surface. So, attenuation correction factor for a particular gamma ray can be simplified as:

$$k_{att} = \frac{1/r^2}{\exp(-\mu_L t)/r^2} \qquad (8)$$

where t is the distance the gamma ray travels in the sample. The exponential term in the denominator corrects for the gamma ray attenuation in the sample. Both ε and t will vary

depending upon the point of origin of the gamma ray in the sample and also on its path followed to reach the detector. In the case of an attenuating container wall, an additional factor in equation 8 in the exponential will come ($\mu_c t_c$, where μ_c and t_c are the linear attenuation coefficient and thickness of the sample wall respectively). As demonstrated below, t_c can be found out by the same procedure as t. Two representative paths of gamma ray originating in a cylindrical sample whose axis is perpendicular to the detector axis are shown in figure 3. Consider the origin is fixed at the centre of gravity of the sample, which lie on the detector axis. Suppose a random point is generated within the sample having co-ordinate (*a, b, c*) and another random point *(a1, d, c1)* on the detector surface which is at a distance d from the origin. Suppose the line connecting (*a, b, c*) and (*a1, d, c1*) intersect the sample cylinder at (*x, y, z*). Then r and t for this representative path is given by:

$$r = \sqrt{(a1-a)^2 + (d-b)^2 + (c1-c)^2} \tag{9}$$

$$t = \sqrt{(x-a)^2 + (y-b)^2 + (z-c)^2} \tag{10}$$

From Eqn. 9, *r* can be calculated since the point of gamma ray origin and the point at which it reaches the detector is known. But for calculating *t*, the co-ordinate of the point of intersection of the line connecting (*a, b, c*) and (*a1, d, c1*) and the sample cylinder i.e. (*x, y, z*) need to be known. The procedure for calculating *(x, y, z)* is given below.

The equation of the straight line joining (*a, b, c*), (*x, y, z*) and (*a1, d, c1*) is given by:

$$\frac{x-a}{a1-a} = \frac{y-b}{d-b} = \frac{z-c}{c1-c} \tag{11}$$

The value of (*x, y, z*) can be obtained from the point of intersection of this straight line and the circle defined by the equation

$$x^2 + y^2 = R^2 \tag{12}$$

where *R* is the radius of the cylindrical sample. Similarly, *r* and *t* can be obtained for any pair of points lying on the detector surface and in the sample volume. In the present numerical approach, a large number of pair of random points is generated which are lying on the detector surface and in the sample volume, the actual k_{att} for the sample will be given by the following equation:

$$k_{att} = \frac{<1/r^2>}{<\exp(-\mu_L t)/r^2>} \tag{13}$$

where <> sign represents the average of the quantity concerned. The approach is hybrid since Monte Carlo principle is combined with analytical method.

4.2. PROGRAMS

A separate FORTRAN program was written for each sample geometry. The programs written for different sample geometries are given below:

4.2.1. Cylindrical geometry

For cylindrical geometry, the attenuation correction program 'CYL.FOR' is given as program 1 in Appendix. In this program, the linear attenuation coefficient (amu or μ) is kept fixed and transmittance of the gamma ray is given as an input in **'transm.txt'**. The input of the program can be changed as required. An example of the input file is given in the input as Input 1 in Appendix. This file gives the list of transmittance of the gamma

ray for which k_{att} values are to be calculated. The corresponding radius of the cylindrical sample is calculated in the program itself. The detector is considered to be cylindrical one, having diameter of 5 cm, which is an input in the calculations. The length of the crystal does not enter in the calculations. The function aphasa is used to generate random numbers in both sample volume and on the detector surface. These co-ordinates are then used to get the intersection point of the gamma ray with the sample surface i.e. (*x, y, z*). Once (*x, y, z*) is known then the distance traveled by the gamma ray in the sample (*t*) and square of the distance traveled by the gamma ray to reach the detector (r^2) is calculated. These are then used to get k_{att}. The output is stored in the file **'cylinder.out'**. The calculations were performed by generating approximately 10^5 particles, using a desktop PC. This program was run separately for different sample-to-detector distances.

4.2.2. Box geometry

Similarly, for a box type sample, the distance traveled by the gamma ray within the sample before reaching the detector (*t*) can be obtained by solving Eq. (11) and the equation defining the plane surface of the box from which the gamma ray is emerging:

$$y = Y \tag{14}$$

where *Y* represents half-thickness of the box. k_{att} can then be obtained from the Eq. 13. The FORTRAN program for box shaped sample 'BOX.FOR' is given as program 2 in Appendix. The symbols and functions used in this program are similar to those used in program 1. The input and the output files are **'transm.txt'** and **'box.out'** respectively. Here also the attenuation correction factors have been calculated as a function of transmittance and sample-to-detector distances. The transmissions were varied by

keeping the linear attenuation coefficient (μ_L) constant and varying the half-thickness of the box (XX or f).

4.2.3. Spherical geometry

For the spherical geometry, the distance traveled by the gamma ray within the sample before reaching the detector can be obtained by solving the Eq. 11 and the following equation defining the spherical surface:

$$x^2 + y^2 + z^2 = R^2 \tag{15}$$

where R is the radius of the sphere. k_{att} can then be obtained from equation 13. The FORTRAN program for spherical sample 'SPHERE.FOR' is given as program 3 in Appendix.

The description of this program is also similar to that of the previous two programs. The input and the output files are **'transm.txt'** and **'sphere.out'** respectively.

4.2.4. Disc geometry

For the disc geometry, the distance traveled by the gamma ray within the sample before reaching the detector can be obtained by solving the Eq. 11 and the following equation:

$$y = f \tag{16}$$

where f is the half-thickness of the disc. k_{att} can then be obtained from Equation 13. The FORTRAN program for disc geometry 'DISC.FOR' is given as program 4 in Appendix. In this program, proper correction for the gamma rays reaching the detector from the walls of the disc has been done. Here, the radius of the cylindrical detector was 3 cm.

This radius was chosen for the calculations to match with the experimental detector dimensions. Separate runs were taken for each sample-to-detector distance.

5. Experimental

Attenuation correction factors were determined experimentally for cylindrical, disc and box geometry. For cylindrical and disc geometry, uranium solution was chosen as the attenuating matrix. For this purpose, nine 20 ml standard uranyl nitrate solutions in the concentration range of 100-390 mg/ml were prepared by dissolving the required amount of U_3O_8 in 2M HNO_3. The cylindrical and disc geometry as explained above in figure 2 was realized by counting the same set of uranyl nitrate samples in a horizontal and a vertical HPGe detector. Both the detectors had a relative efficiency of 20% and a resolution of 2.2 keV at 1.33 MeV. The gamma rays emitted by U-235 in the range of 143-205 keV were monitored. The efficiency of the required geometry was obtained by using 20 ml Eu-152 and Ba-133 standard solutions. Out of the nine samples, the attenuation correction factors were determined for the four samples with highest uranium concentration.

The linear attenuation coefficient μ_L (cm^{-1}) which is required as an input for the present numerical approach was measured experimentally for all the four samples at the energies of interest, by transmission measurement of a collimated beam. For this, the sample was counted with and without the transmission source. Figure 1 shows the schematic of experimental set-up. The ^{169}Yb was used as the transmission source as it has gamma rays close to the ^{235}U gamma rays used in our measurement. Table 1 gives the ^{169}Yb gamma ray energies and their corresponding abundances used for transmission measurement.

Here, the unattenuated count rate was obtained by replacing the sample with 2M HNO_3. The transmission curve as a function of gamma ray energy is shown in figure 4. The highlighted points in the figure shows the gamma ray energies of ^{235}U monitored. The transmittance for ^{235}U energies was obtained by linear interpolation between the transmittance for ^{169}Yb energies. The linear attenuation coefficient is then obtained from Eq. 4.

For box shaped samples, lead acetate solutions were used as the attenuating matrix, keeping in mind the high Z of lead and high solubility of lead acetate. These solutions in the concentration range of 10 - 400 mg/ml were prepared by dissolving required amount of lead acetate in water. The linear attenuation coefficients of these samples were measured by using ^{57}Co as the transmittance source by the method described above. To get experimental attenuation correction factors, known amount of ^{57}Co activity was added to the samples. Known amount of activity was also added to a water sample which was chosen as a blank. These samples along with the blank were then counted in a 20% HPGe with a resolution of 2.2 keV at 1332 keV.

6. Results and Discussion

Figure 5 shows the experimental disintegration rate corresponding to different energies as a function of uranium concentration for cylindrical geometry. These were calculated by using the standard formula:

$$dps_{expt} = \frac{CR_\gamma}{\varepsilon_\gamma \, a_\gamma} \qquad (17)$$

where, CR_γ, ε_γ, a_γ is the count rate from sample, efficiency and abundance of the gamma ray concerned. The straight line in the figure is the calculated dps of the U-solution obtained from the known uranium concentration. It can be seen from the figure that the experimental dps deviates from linearity. This deviation increases with the U-concentration and with the decreasing gamma ray energy. This clearly points to the effect of gamma ray attenuation by the U-solutions. Thus, the actual dps of the solution can be obtained from experimental dps as given below:

$$dps = dps_{\exp t} \times k_{att} \qquad (18)$$

where k_{att} is the attenuation correction factor. So, experimental k_{att} can be obtained from the ratio of theoretical dps to the experimental dps.

Figure 6 shows the experimental count rate per gram for ^{57}Co activity as a function of lead acetate concentration for box samples. The straight line in the figure shows the expected count rate per gram as a function of lead acetate concentration. Here also, due to gamma ray attenuation, there is a deviation from linearity as lead acetate concentration increases.

6.1 Validation of the present approach by MCNP and analytical models available in literature

The present approach was validated by comparing its results with MCNP calculations and geometrical formulae available in literature. The comparison was done at all sample-to-detector distance and for all degrees of attenuation. Three most commonly used sample geometries namely sphere, box and cylindrical were considered. As a first step, all the calculations were done by keeping the sample-to-detector distance sufficiently large so

that the results can be compared with the far-field correction factors available in the literature. In the case of cylinder, the height was of the order of the diameter of the detector so that the path of the gamma ray reaching the detector from the top or bottom surface could be neglected. But practically, if the height of the sample to be analyzed is such that the there is a finite probability of gamma rays reaching the detector from the top or bottom of the sample, then the corrections can be easily incorporated in the required program. Table 2 gives the results of the present k_{att} calculations for the three geometries using a sample-to-detector distance of 100 cm. It also gives the corresponding k_{att} values calculated from the following far-field analytical expressions [1]:

$$k_{att(cylinder)} = \frac{1}{2}\frac{\mu D}{[I_1(\mu D) - L_1(\mu D)]} \tag{19}$$

$$k_{att(box)} = \frac{\mu x}{[1-\exp(-\mu x)]} \tag{20}$$

$$k_{att(sphere)} = (\frac{3}{2}\{1 - \frac{2}{(\mu D)^2} + \exp(-\mu D)\left[\frac{2}{\mu D} + \frac{2}{(\mu D)^2}\right]\})^{-1} \tag{21}$$

where D is the diameter of the cylinder and sphere, x is the half-thickness of the box, I_1 and L_1 are modified Bessel and modified Struve functions of order 1. The data in Table 2 show a good agreement between the present calculations and the literature for all geometries, but deviations up to 5% are observed at very low transmittance. This validates the method of our calculation of k_{att} at far-field geometry.

In order to get an idea about the minimum sample-to-detector distance upto which far-field expressions available in literature can be applied, present calculations for all the three geometries were performed at varying sample-to-detector distance. These results were compared with the result of calculation from literature formula. Figure 7(a) shows the ratio of k_{att} obtained by the present calculations to the k_{att} calculated from the far-field expressions at different sample-to-detector distances for cylindrical geometry. The results agree within 2% at almost all transmittance at higher distance (> 50 cm). The deviation starts at lower distance, particularly at lower transmittance. The lower value of k_{att} than predicted by far-field expression is expected at closer distance as the geometric efficiency becomes dependent on the position of emission of gamma ray within the sample. In order to further confirm the result of the present calculations, Monte Carlo simulation for the given sample-detector geometry were performed using MCNP code. For this purpose, company supplied dimension of the detector was used and a uranium solution of known concentration having experimentally determined μ_L = 0.5 cm^{-1} at 186 keV was chosen as the matrix. The transmittance of the solution was varied by changing the radius of the cylinder. The unattenuated count rate was obtained by replacing the sample solution by air. The k_{att} was calculated from the ratio of unattenuated to attenuated count rates. The results of the present calculations relative to MCNP calculations for cylindrical geometry are shown in figure 7(b). It is observed that the ratio no longer shows the kind of distance dependence as observed in figure 7(a). This shows that the result of our calculations is applicable at all sample-to-detector distance. However, the ratio in figure 7(b) shows about 10% deviation at lowest transmittance independent of sample-to detector distance. This may be due to inherent uncertainty involved in the MCNP calculations.

To see whether the present calculation converges with the prediction of near-field formula, these results were compared with the results of near-field expressions (two-dimensional model) as given below [1] for cylindrical geometry:

$$k_{att} = \frac{\sum_{m=1}^{M}\sum_{n=1}^{N} \Delta A(m,n)/L^2(m,n)}{\sum_{m=1}^{M}\sum_{n=1}^{N}\left\{\exp\left[-\mu t(m,n)\right]\right\}\Delta A(m,n)/L^2(m,n)} \qquad (22)$$

where $\Delta A(m,n)$ is the area element of a circular cross-section of the sample, $L(m,n)$ is the distance of the area element from the point detector, $t(m,n)$ is the distance traveled by the gamma ray in the sample. Figure 8(a) shows the two-dimensional model k_{att} relative to k_{att} values obtained from far-field expressions. Here also, it was observed that the near-field formula match reasonably well at longer distances at all transmittance with the far-field values and as expected, the deviation starts at shorter sample-to-detector distance at lower transmittance. The increasing importance of geometric efficiency at less sample-to-detector distance is apparent from the increasing deviation of far-field formula from near-field values as the distance decreases. The comparison of the present result with the two dimensional model has been shown in figure 8(b). It is observed that the values match within 2 % at all transmittance even at 10 cm sample-to-detector distance. The deviation observed at shorter distance may indicate the failure of the near-field formula at very close sample-to-detector distance and needs further investigation. For quantitative comparison, the k_{att} values at 10, 5 and 3.5 cm sample-to-detector distance, calculated based on two-dimensional model, present calculations and MCNP calculations are given in Table 3. As seen from the table, there is excellent agreement of the results of all the three calculations but for lowest transmittance values where agreement is seen between

the present calculation and MCNP. Thus, it is seen that the present method is independent of any approximations regarding sample-to-detector distance for calculating k_{att} for cylindrical geometry.

Similar calculations were performed for box and spherical geometry. Figure 9(a) shows the comparison of the present calculation with far-field expressions for box geometry. Again, the deviation from the literature expression is observed at lower transmittance and at shorter distance. The corresponding results with respect to MCNP simulation are shown in figure 9(b). The distance dependence of the deviation, as seen from figure 9(a) disappears in figure 9(b). Also, the predictions of MCNP agree within 5-8 % with our results at all distance and at all transmittance. Similar comparisons are shown in figure 10 (a) and (b) for spherical geometry. In this case, the results of our calculations and far-field formula agree within 1 % for all transmittance at all distance except at highest transmittance and 5 cm distance. The MCNP results also show the similar trend. It appears that the far-field formula for spherical geometry is applicable at all sample-to-detector distance in the transmittance range considered in the present work. It is thus seen that the k_{att} values for common sample geometries, at all sample-to-detector distance, and in the transmittance range considered, can be calculated using the common approach developed in the present work. The MCNP calculations also provide a good estimate of the k_{att}. However, the calculations are involved, time-consuming and require full description of the detector geometry and exact sample composition. The present calculations are simple, rapid and require only μ_L, detector diameter and sample dimensions as input. The calculations can be extended to disc-shaped and other common

geometries. The calculations will be particularly useful for attenuation corrections at shorter sample-to-detector distance where analytical formulae are not available.

6.2 Experimental validation of the hybrid Monte Carlo approach

6.2.1 Cylindrical samples

To further validate the present attenuation correction procedure developed, the results of the present calculations were compared with the experimentally determined k_{att}. For this, the experimental disintegration rates of a particular uranyl nitrate sample at the energy of interest (143 and 186 keV) was obtained by correcting the measured count rate of the sample with the efficiency at that energy and the intensity of the corresponding gamma ray. For efficiency calibration, ^{152}Eu and ^{133}Ba were used in the same geometry. The experimental disintegration rates as said before will not be constant for a particular sample and will show the increasing effect of attenuation as the gamma ray energy decreases. The experimental k_{att}'s at a particular energy was then determined by taking the ratio of the actual disintegration rate of the sample and the experimental disintegration rate at that energy. These measurements were also carried out at different sample-to-detector distances so as to check the applicability of the current approach over a wide range of sample-to-detector distances.

To calculate the attenuation correction factors from the numerical method, the sample dimensions and sample-to-detector distance were given as an input in the calculations. In all the calculations, the sample diameter and height were taken to be 2.54 cm and 4 cm respectively. The detector diameter was 5 cm for horizontal detector (cylindrical geometry) and 6 cm for vertical detector (disc geometry). Along with this, the linear

attenuation coefficients obtained experimentally at the energies monitored for different samples were given as an input in the program. These calculations were also performed by generating approximately 10^5 particles, using a desktop PC.

To further confirm the result of the present calculations, Monte Carlo simulation for both the geometries was performed using MCNP code. In these calculations, apart from the precise information about the sample-detector geometry, the concentration of uranium in the sample was given as an input. The unattenuated count rate was obtained by replacing the sample solution by air. The k_{att} from MCNP was calculated from the ratio of unattenuated to attenuated count rates. Figure 10 shows the theoretical k_{att} values calculated from the given method compared with the experimental and MCNP results for cylindrical geometry at d = 2.5, 4.5 and 20 cm as a function of transmittance. It is seen from the figure that at d = 4.5 and 20 cm, the experimental and the MCNP k_{att} values matches well with the present method k_{att} and with the near-field formula. But at d = 2.5 cm, the near-field values shows a deviation from the experimental and the MCNP k_{att} values but the present approach values matches well. This shows that the near-field formula is not valid at very near sample-to-detector distances while the present calculation is valid at all sample-to-detector distances.

Figure 12 shows the comparison of theoretical, experimental and MCNP obtained k_{att} values for disc geometry at three sample-to-detector distances, d = 2, 4, 5 cm. Here also, the theoretical values match reasonably well with the MCNP and experimental k_{att} values at all the distances. This validates the numerical approach explained above over a wide range of sample-to-detector distances. Figure 12 also shows the k_{att} values calculated from a near-field one dimensional model given in [1] :

$$CF(AT) = \left[\frac{D}{d(d+D)} \right] \Bigg/ \sum_{I=1}^{N} \frac{\{\exp[-\mu(I-0.5)\Delta x]\}\,\Delta x}{[d+(I-0.5)\Delta x]^2} \qquad (23)$$

Here Δx = D/N where D is the sample depth, N is the number of intervals for the numeric integration and d is the distance from the sample surface to the detector surface. The model approximates the sample to be a line sample of depth 'D' and detector to be a point detector. As seen from the figure, the near-field formula values deviates significantly at very close sample-to-detector distance i.e. when the sample is almost in the touching configuration with the detector. This implies that the near-field formula although said to be valid at close sample-detector geometry, starts working only after certain sample-to-detector distance, whereas the numerical approach is found to be applicable at all sample-to-detector distance.

6.2.2 Box-shaped samples

For box samples, experimental k_{att} were determined by taking the ratio of count rate per gram of blank to the count rate per gram of sample. These k_{att} were compared with the far-field k_{att} as given by equation 21 and with the k_{att} calculated from present approach. Figure 13 shows the experimental, far-field and present method k_{att} for box-shaped sample at sample-to-detector distances, d = 2.6, 5.0 and 20.1 cm. As expected, at close distance i.e. at d = 2.6 and 5.0 cm, the experimental k_{att} deviates significantly from far-field values but matches quite well with the present approach k_{att}. When the sample-to-detector distance is 20.1 cm, all the three attenuation correction factors match well. This again shows that the present approach is valid at all sample-to-detector distances.

Conclusion

A hybrid Monte Carlo method has been developed for calculations of attenuation correction factors for samples of varied geometries. The results of the present calculation show the possibility of using a simplified common approach to calculate the k_{att} for the simple geometries considered, over wide range of transmittance. A comparison with experimental measurements has also been done to validate the results of these calculations, particularly at closer sample-to-detector distance. It was observed that the near-field formulas available in literature are applicable only after certain sample-to-detector distance. The advantage of the numerical method is that it is free of any assumptions regarding sample-detector geometry. Also, the present approach is common to all sample geometries and sizes. The present calculation can also be extended to other geometries.

References:

1. D. Reilly, N. Ensslin, H. Jr. Smith, S. Kreiner, 1991. Passive Nondestructive Assay of Nuclear Materials, Los Alamos National Laboratory, United States.
2. “Self-Shielding correction for Photon Irradiation of Slab and Cylindrical Samples”, Gulf General Atomic, Inc.,Progress Report GA-9614 (1969).
3. J. P. Francois , Nucl. Instr. and. Meth. 117 (1974) 153.
4. L. Moens, J. De Donder, Lin Xilei, F. De Corte, A. De Wispelaere, A. Simonits, J. Hoste, Nucl. Instr. and. Meth. 187 (1981) 451.
5. K. Debertin, R. E. N. Jianping, Nucl. Instr. and. Meth. A, 278 (1989) 541.
6. S. Yalcin, O. Gurler, G. Kaynak, O. Gundogdu, Appl. Radiat. Isot, 65 (2007) 1179.
7. I. Badawy, A. S. Youssef, SH. El-Kazzaz, W. A. El-Gammal , Nucl. Instr. and. Meth. A453 (2000) 621.
8. J.F. Briesmeister, 2000. MCNP – a general Monte Carlo N-particle transport code version 4C LA-13709-M, Los Alamos National Laboratory, USA.
9. C. Agarwal, S.Poi, A.Goswami, Nucl. Instr. and. Meth. A (In Press).

Table 1. Gamma ray energies of ^{169}Yb and ^{235}U .

Gamma ray energy (keV)	
^{169}Yb	^{235}U
130.5	143.8
177.2	163.4
198.0	185.7
307.7	205.3

Table 2. Results of k_{att} calculations by the present method and comparison with values available in the literature for samples of different geometries.

	Cylinder		Box		Sphere	
Transmittance	k_{att}	k_{att}*	k_{att}	k_{att}*	k_{att}	k_{att}*
0.01	3.74	3.79	4.43	4.65	3.36	3.37
0.09	2.29	2.30	2.60	2.65	2.10	2.11
0.17	1.90	1.91	2.11	2.13	1.78	1.78
0.25	1.68	1.69	1.84	1.85	1.59	1.59
0.33	1.53	1.54	1.65	1.65	1.46	1.46
0.41	1.42	1.42	1.51	1.51	1.36	1.37
0.57	1.25	1.26	1.31	1.31	1.22	1.22
0.73	1.14	1.14	1.17	1.17	1.12	1.12
0.89	1.05	1.05	1.06	1.06	1.04	1.04
0.97	1.01	1.01	1.02	1.02	1.01	1.01

*From ref [1]

Table 3. Results of k_{att} calculations by the present method and comparison with values available in the literature and MCNP values for cylindrical sample.

Transmittance	*d* = 10cm			*d* = 5cm			*d* = 3.5cm*		
	$k_{att}^{\$}$	$k_{att}^{\#}$	$k_{att}^{\&}$	$k_{att}^{\$}$	$k_{att}^{\#}$	$k_{att}^{\&}$	$k_{att}^{\$}$	$k_{att}^{\#}$	$k_{att}^{\&}$
0.01	3.09	3.17	3.05	2.03	2.76	2.79	2.27	3.10	3.06
0.09	2.16	2.19	2.10	2.00	2.12	2.06	2.03	2.22	2.13
0.17	1.84	1.86	1.80	1.77	1.83	1.78	1.78	1.89	1.82
0.25	1.65	1.66	1.61	1.61	1.65	1.61	1.62	1.69	1.63
0.33	1.51	1.52	1.49	1.49	1.52	1.48	1.49	1.55	1.50
0.41	1.41	1.42	1.39	1.39	1.42	1.39	1.40	1.44	1.40
0.57	1.25	1.25	1.24	1.25	1.26	1.24	1.25	1.27	1.25
0.73	1.14	1.14	1.13	1.14	1.14	1.13	1.14	1.15	1.14
0.89	1.05	1.05	1.05	1.05	1.05	1.05	1.05	1.05	1.05
0.97	1.01	1.01	1.01	1.01	1.01	1.01	1.01	1.01	1.01

$^{\$}$ From 2D model

$^{\#}$ From present calculations

$^{\&}$ From MCNP calculations

* These calculations were done with a higher μ so as to reduce the radius of the sample so that sample does not overlap with the detector.

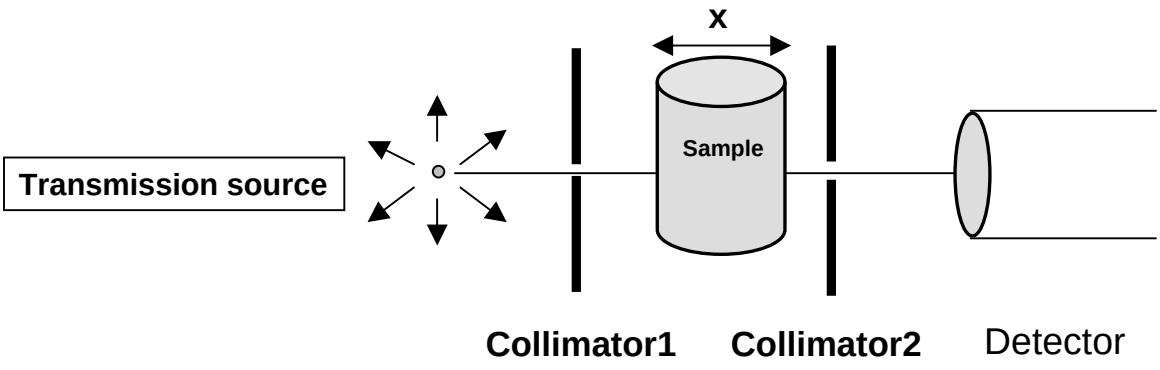

Figure 1. The experimental set up for the measurement of linear attenuation coefficient (μ_L) by transmission technique.

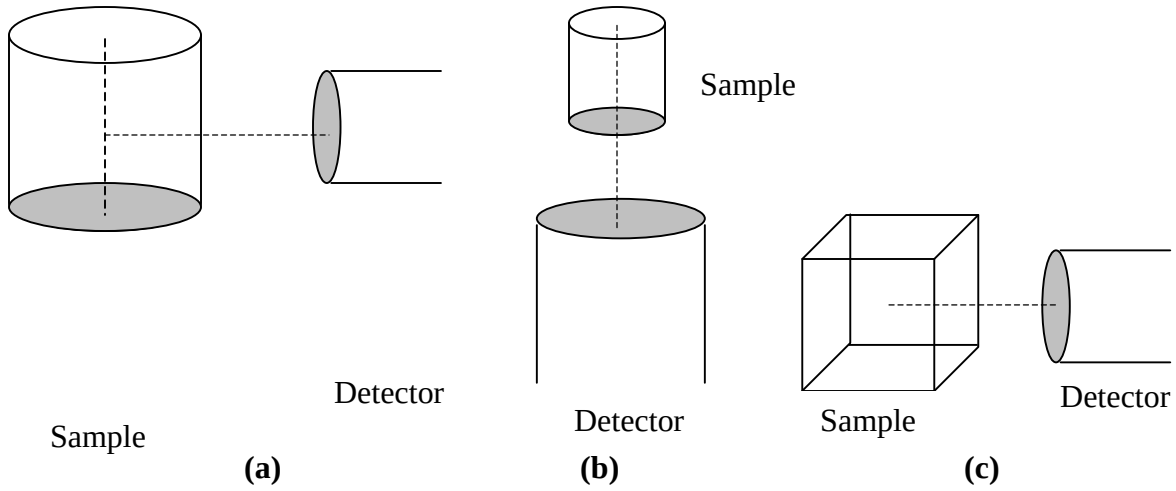

Figure 2. The geometrical arrangement of the sample and detector. **(a)** Cylindrical geometry **(b)** Disc geometry and **(c)** Box geometry.

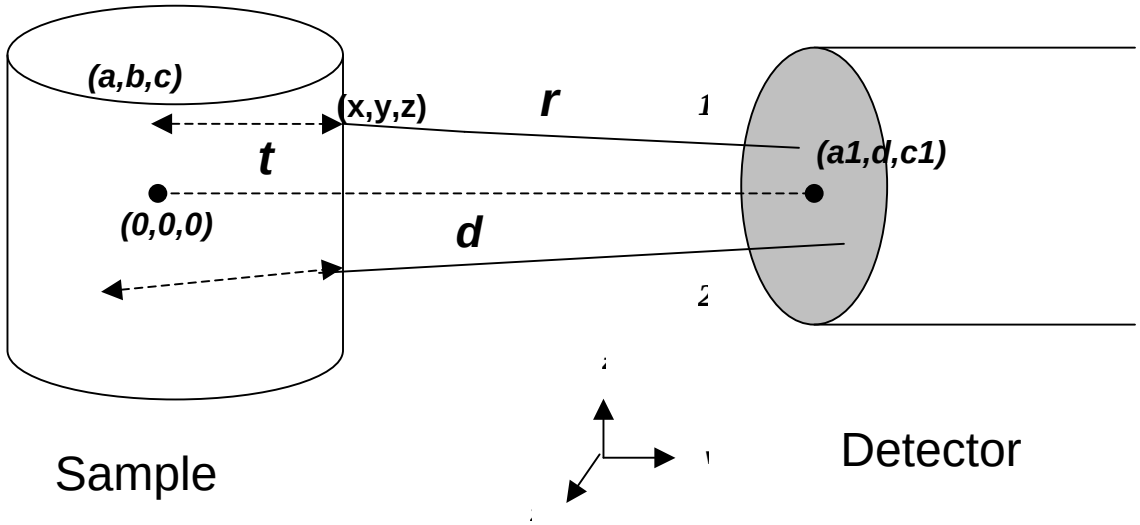

Figure 3. Representative paths of two gamma rays from sample to the detector surface.

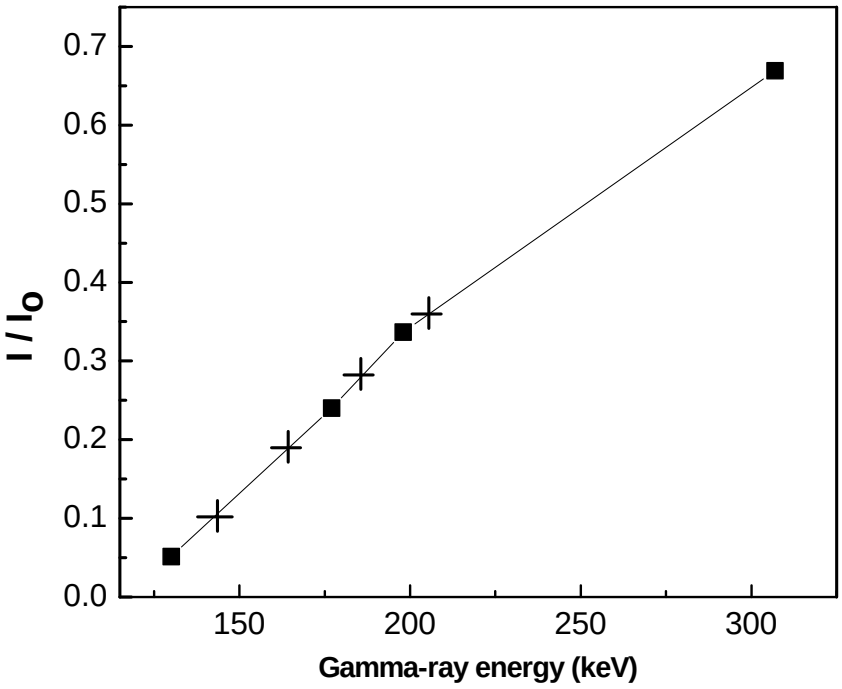

Figure 4. Transmission curve as a function of gamma ray energy using ^{169}Yb as transmission source.

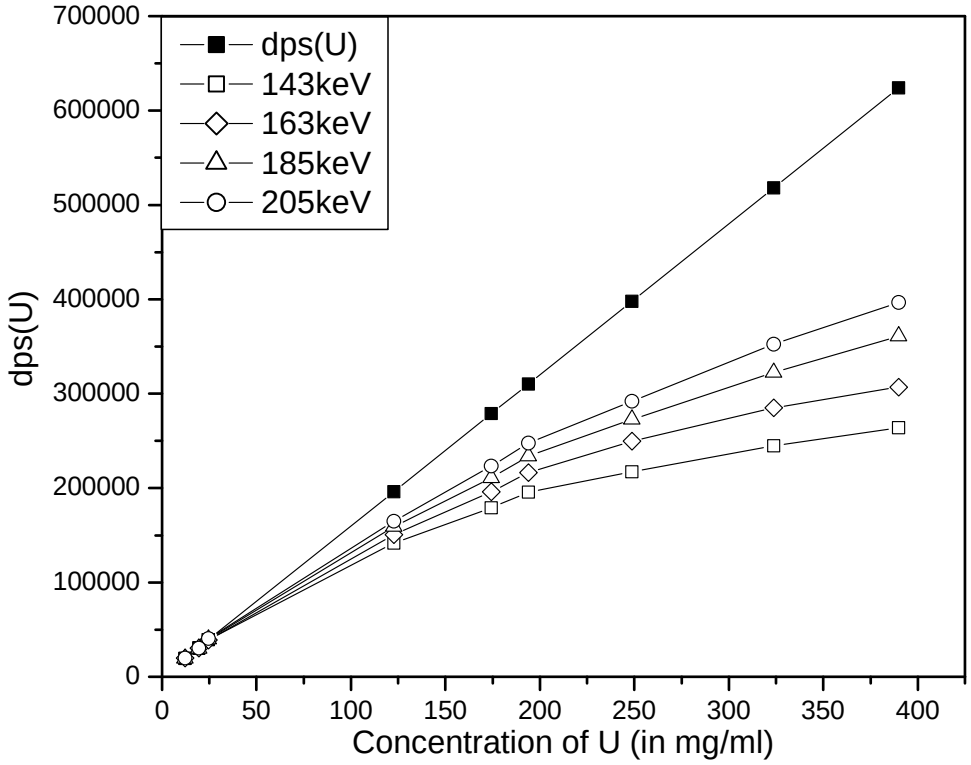

Figure 5. Disintegration rate of uranium at different energies as a function of uranium concentration. The straight line shows the expected dps from the samples as a function of uranium concentration.

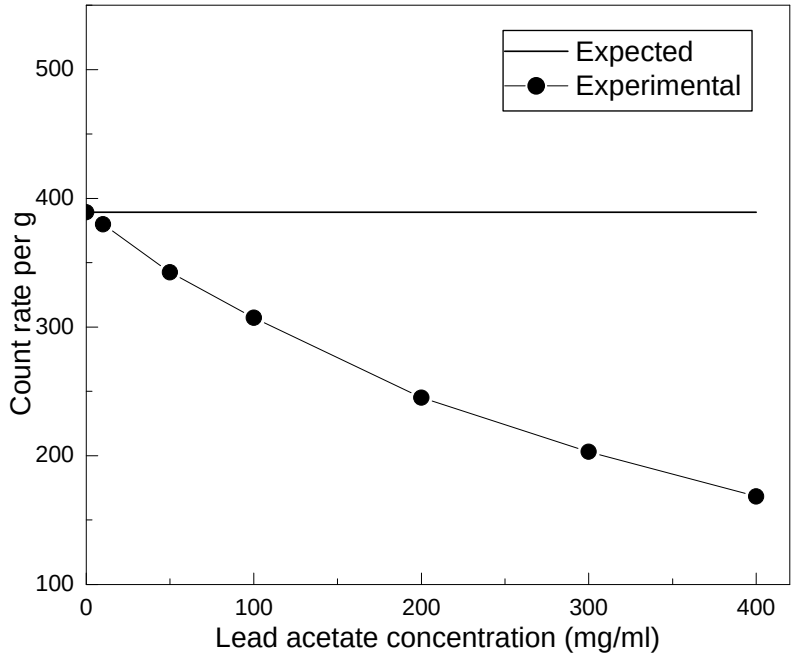

Figure 6. Count rate per gram of Co-57 activity at 122 keV as a function of lead acetate concentration. The straight line shows the expected count rate per gram as a function of lead acetate concentration.

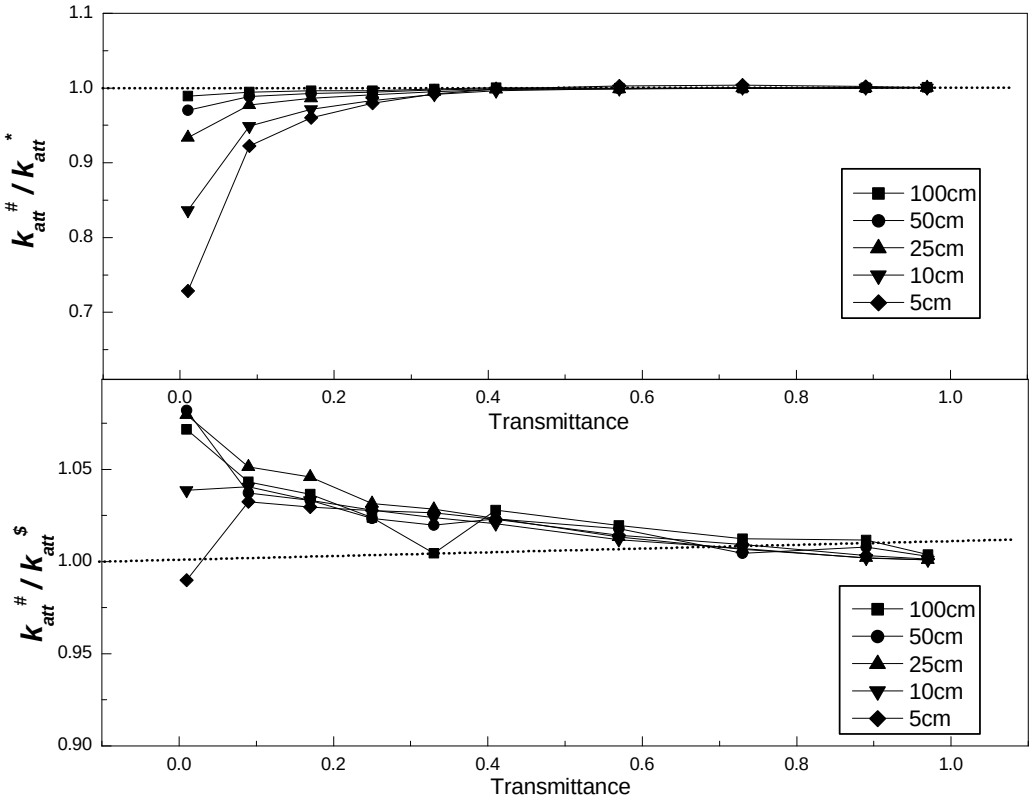

Figure 7. Ratio of attenuation correction factors at different distances as a function of transmittance for cylindrical geometry. (a) $k_{att}^{\#} / k_{att}$*

(b) $k_{att}^{\#} / k_{att}^{\$}$

[#] Present calculation

[$] MCNP calculation

[*] From Ref[1]

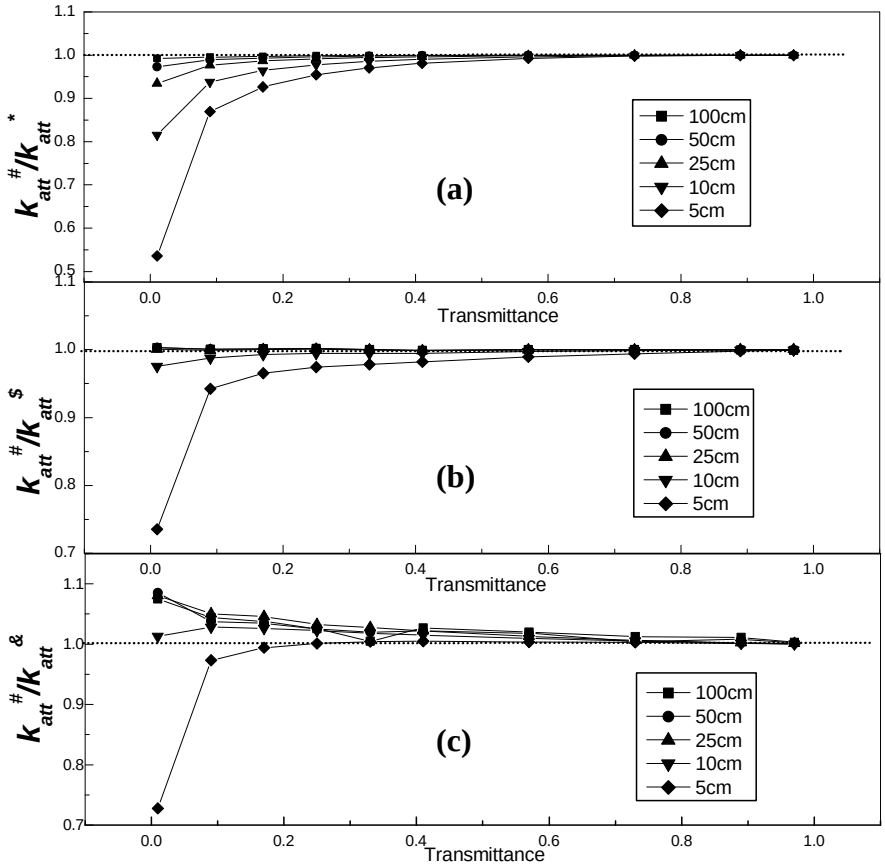

Figure 8. Ratio of attenuation correction factors at different distances as a function of transmittance for cylindrical geometry. (a) $k_{att}^{\#} / k_{att}$*

(b) $k_{att}^{\#} / k_{att}^{\$}$

(c) $k_{att}^{\#} / k_{att}^{\&}$

[#] Two-dimensional model[1] calculation

[$] Present calculation

[*] From Ref.[1]

[&] From MCNP calculations

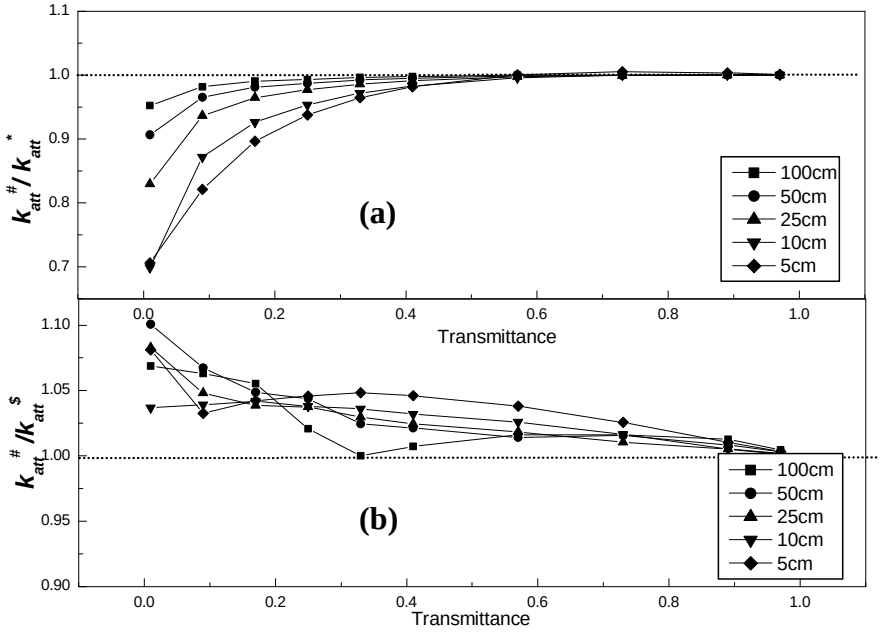

Figure 9. Ratio of attenuation correction factors at different distances as a function of transmittance for box-shaped sample. (a) $k_{att}^{\#} / k_{att}^{*}$

(b) $k_{att}^{\#} / k_{att}^{\$}$

$^{\#}$ Present calculation

* From Ref[1]

$^{\$}$ MCNP calculation

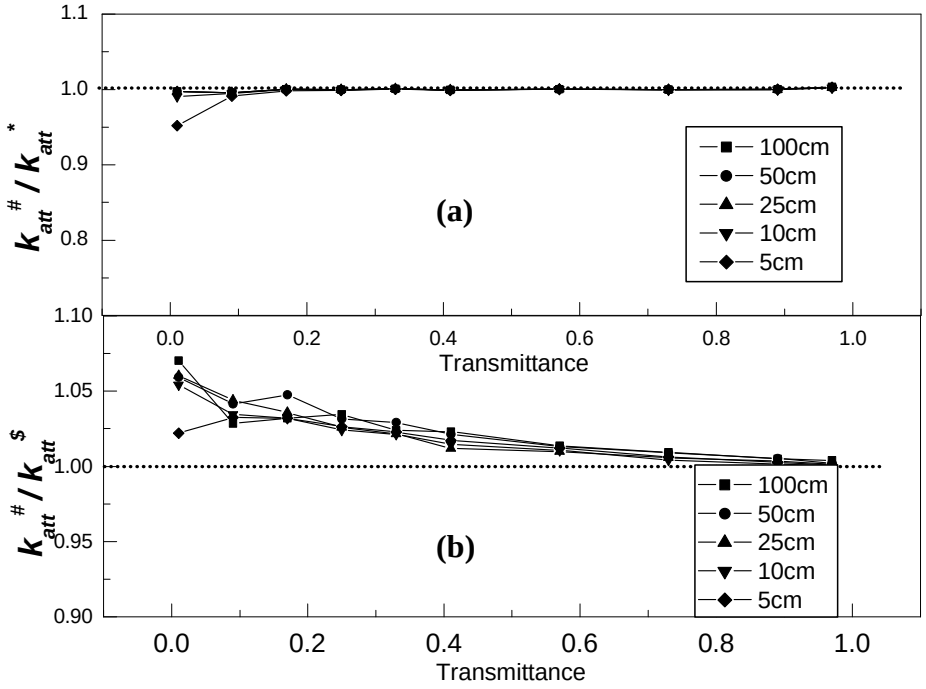

Figure 10. Ratio of attenuation correction factors at different distances as a function of transmittance for spherical geometry. (a) $k_{att}^{\#} / k_{att}^{*}$

(b) $k_{att}^{\#} / k_{att}^{\$}$

$^{\#}$ Present calculation

* From Ref[1]

$^{\$}$ MCNP calculation

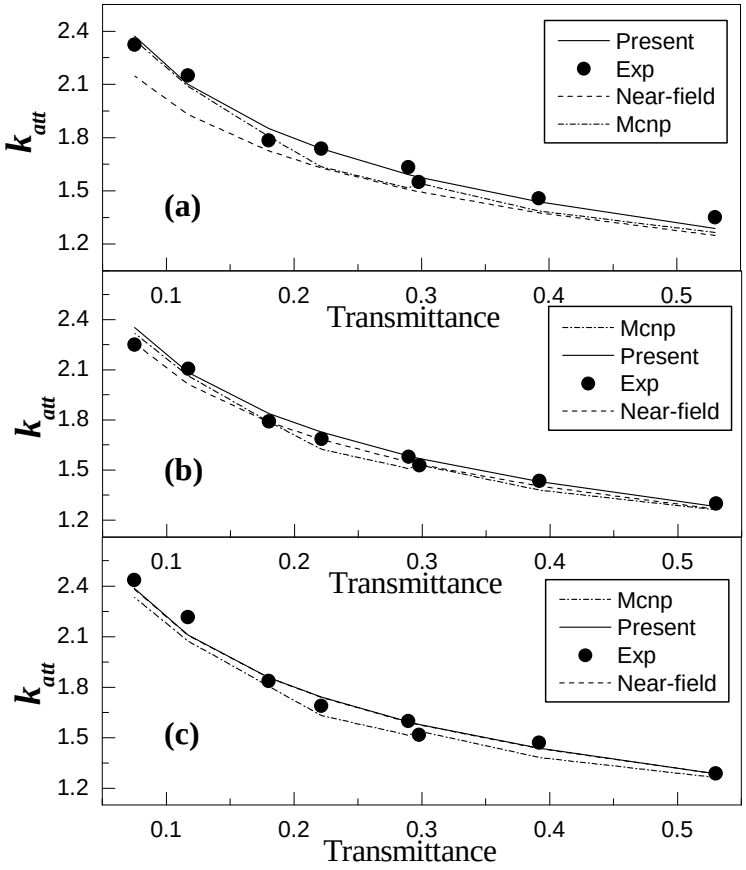

Figure 11. The attenuation correction factors computed using numerical approach for cylindrical geometry as a function of transmittance for different sample-to-detector distances (d) **a)** d = 2.5 cm. **b)** d = 4.5 cm. **c)** d = 20 cm.

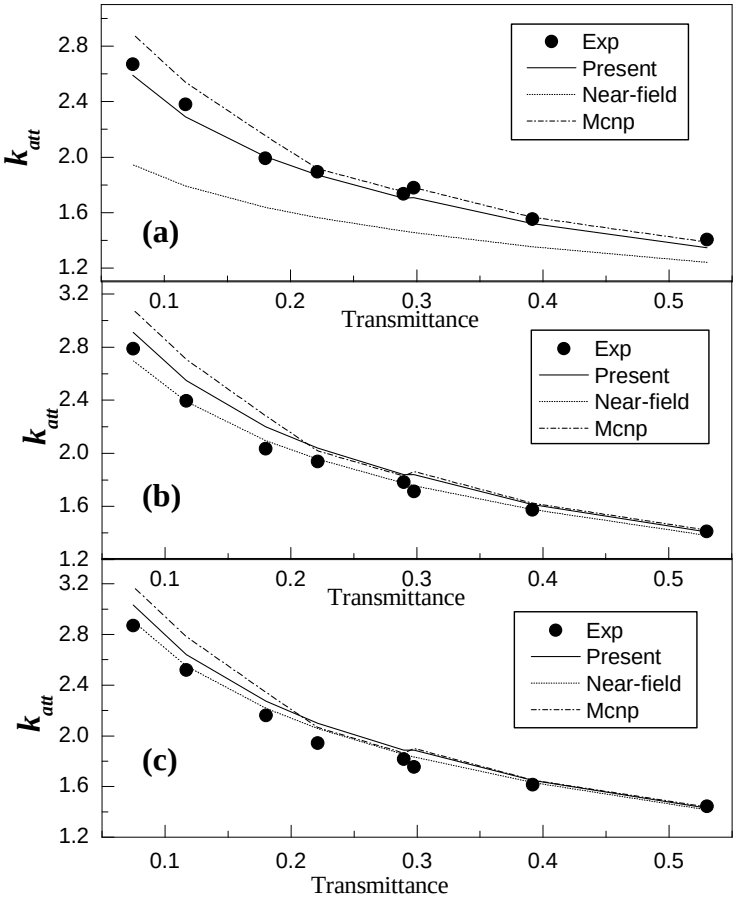

Figure 12. The attenuation correction factors computed using numerical approach for disc geometry as a function of transmittance for different sample-to-detector distances (d) **a)** d = 2 cm. **b)** d = 4 cm. **c)** d = 5 cm.

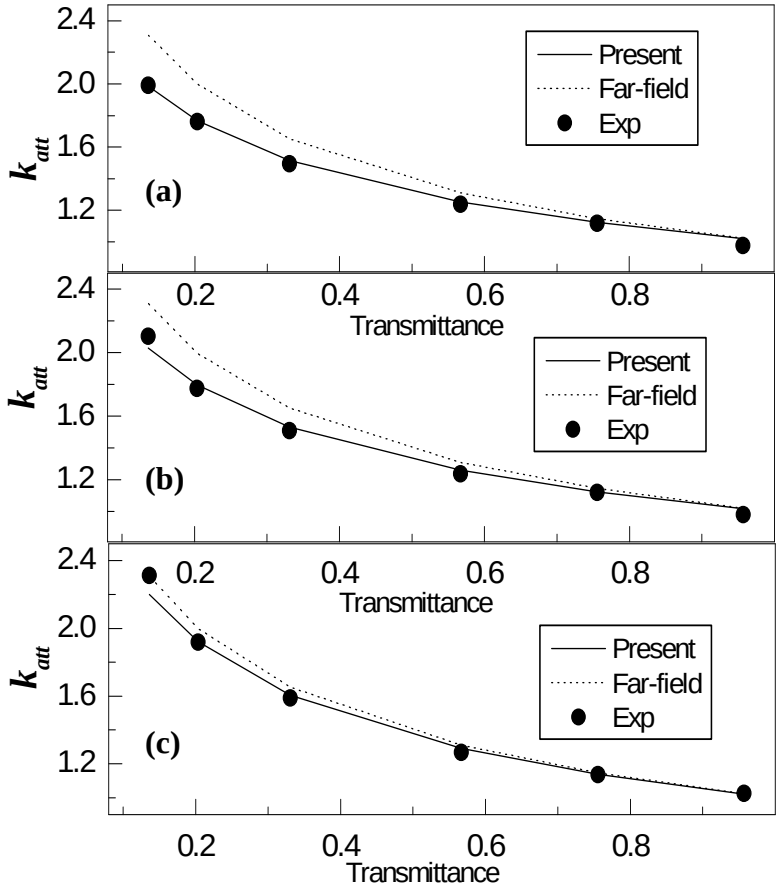

Figure 13. The attenuation correction factors computed using numerical approach for box geometry as a function of transmittance for different sample-to-detector distances (d) **a)** d = 2.6 cm. **b)** d = 5.0 cm. **c)** d = 20.1 cm.

APPENDIX

Program 1.

```
c ***************************************************************
cc --- Attenuation correction factors for cylindrical geometry -------
c ***************************************************************
c        //// DESCRIPTION OF THE PARAMETERS ////
c        N = Number of input transmittance value for which attenuation
c        correction factor has to be calculated
c        h = Half - height of the cylinder
c        nmax = number of random points generated
c        d = sample to detector distance taken from the centre of the sample
c        amu = linear attenuation coefficient
c        tt = transmittance
c        r, f = radius of cylinder
c        dr = radius of detector crystal
c        CFAT = Attenuation correction factor
c        //// ALL THE QUANTITIES ARE IN CGS UNITS. ////
         N = 10
         nmax = 100000
c        //// OPENING AN INPUT AND OUTPUT FILE ////
         open (9 ,file = 'transm.txt')
         open (8, file = 'cylinder.out')
         h = 2.0
         d = 100.0
         dr = 2.5
         amu = 0.502294
c        //// READING THE INPUT FILE ////
         do 20 k = 1, N
         read (9,*) tt
         alnt = alog (tt)
c        //// CALCULATION OF SAMPLE RADIUS ////
         f = (-alnt/amu/2.0)
         r = f
         sum1 = 0.
         sum2 = 0.
         do 10 i = 1, nmax
c        //// GENERATION OF RANDOM POINTS IN SAMPLE VOLUME ////
         a = aphasa (-f, f)
         b = aphasa (-f, f)
         c = aphasa (-0.0, h)
         bb=sqrt (a*a + b*b)
         if (bb.gt.r) goto 10
c        //// GENERATION OF RANDOM POINTS ON DETECTOR SURFACE ////
         a1 = aphasa (-dr, dr)
         c1 = aphasa (-dr, dr)
```

```
      aaa = sqrt (a1*a1+c1*c1)
      bbb = dr
      if (aaa.gt.bbb) goto 10
c     //// CALCULATION OF (X,Y,Z) ////
      p = (d-b)**2+(a1-a)**2
      q = -2.0*(a1-a)*(b*a1-a*d)
      s = f**2*(d-b)**2
      s = -(s-(b*a1-a*d)**2)
      y1 = q*q-4.0*p*s
      y = (-q+sqrt(y1))/(2.0*p)
      z = (y*(c1-c)-b*c1+c*d)/(d-b)
      x = (y*(a1-a)-b*a1+a*d)/(d-b)
c     //// CALCULATION OF NUMERATOR AND DENOMINATOR OF EQN 13 ////
      t = sqrt((b-y)**2+(c-z)**2+(a-x)**2)
      rsquare = ((b-d)**2+(c-c1)**2+(a-a1)**2)
      term = (exp(-amu*t))/rsquare
      sum1 = sum1+(1./rsquare)
      sum2 = sum2+term
10    continue
c     //// ATTENUATION CORRECTION FACTOR CALCULATION ////
      cfat = sum1/sum2
      print *,cfat, tt, f
c     //// WRITING THE OUTPUT IN FILE ////
      write (8,*) tt, f, cfat,
20    continue
      end
      Function aphasa(x1, x2)
c     aphasa
c     random floating point number equally distributed between x1 and x2
      double precision a,b
      data a /.78149275363e0/
      b = (a+11d0/87d0)*87d0
      i = b
      a = b-i
      aphasa = x1+(x2-x1)*a
      return
      end
```

Input 1. “transm.txt”

```
.01
.09
.17
.25
.33
.41
.57
.73
.89
.97
```

Program 2.

```
c ***************************************************************
cc --- Attenuation correction factors for box geometry -------
c ***************************************************************
c       //// DESCRIPTION OF THE PARAMETERS ////
c       N = Number of input transmittance value for which attenuation
c       correction factor has to be calculated
c       nmax = number of random points generated
c       d = sample to detector distance taken from the centre of the sample
c       amu = linear attenuation coefficient
c       tt = transmittance
c       yy, f = half thickness of box
c       dr = radius of detector crystal
c       CFAT = Attenuation correction factor
c       //// ALL THE QUANTITIES ARE IN CGS UNITS. ////
        N = 10
        nmax = 100000

 c      //// OPENING AN INPUT AND OUTPUT FILE ////
        open(8, file='transm.txt')
        open(9, file='box.out')
        amu= 0.502294
        d=100.0
c       //// READING THE INPUT FILE ////
        do 20 k=1, N
        read (8,*)tt
        alnt = alog(tt)
c      //// CALCULATION OF SAMPLE HALF-THICKNESS ////
        f = -alnt/amu/2.0
        yy = f
        sum1 = 0.
```

```
      sum2 = 0.
      do 10 i = 1, nmax
c     //// GENERATION OF RANDOM POINTS IN SAMPLE VOLUME ////
      a= aphasa(0.0, f)
      b = aphasa(-f, f)
      c = aphasa(0.0, f)
c     //// GENERATION OF RANDOM POINTS ON DETECTOR SURFACE ////
      a1 = aphasa(-dr, dr)
      c1 = aphasa(-dr, dr)
      aaa = sqrt (a1*a1+c1*c1)
      bbb = dr
      if (aaa.gt.bbb) goto 10
c     //// CALCULATION OF (X,Y,Z) ////
      z=(yy*(c1-c)-b*c1+c*d)/(d-b)
      x=(yy*(a1-a)-b*a1+a*d)/(d-b)
c     //// CALCULATION OF NUMERATOR AND DENOMINATOR OF EQN 13 ////
      t=sqrt((b-yy)**2+(c-z)**2+(a-x)**2)
      rsquare=((b-d)**2+(c-c1)**2+(a-a1)**2)
      term=(exp(-amu*t))/rsquare
      sum1=sum1+(1./rsquare)
      sum2=sum2+term
10    continue
c     //// ATTENUATION CORRECTION FACTOR CALCULATION ////
      cfat=sum1/sum2
      print *,tt, f, cfat
c     //// WRITING THE OUTPUT IN FILE ////
      write(9,*)tt, f, cfat
20    continue
      end
      function aphasa(x1,x2)
c     aphasa:
c     random floating point number equally distributed between x1 and x2
      double precision a,b
      data a /.78149275363e0/
      b=(a+11d0/87d0)*87d0
      i=b
      a=b-i
      aphasa=x1+(x2-x1)*a
      return
      end
```

Program 3.

```
c ***************************************************************
cc --- Attenuation correction factors for spherical geometry -------
c ***************************************************************
c       //// DESCRIPTION OF THE PARAMETERS ////
c       N = Number of input transmittance value for which attenuation
c       correction factor has to be calculated
c       nmax = number of random points generated
c       d = sample to detector distance taken from the centre of the sample
c       amu = linear attenuation coefficient
c       tt = transmittance
c       r, f = radius of sphere
c       dr = radius of detector crystal
c       CFAT = Attenuation correction factor
c       //// ALL THE QUANTITIES ARE IN CGS UNITS. ////
        N = 10
        nmax = 100000
 c      //// OPENING AN INPUT AND OUTPUT FILE ////
        open (8,file = 'transm.txt')
        open (9,file = 'sphere.out')
        d = 100.0
        amu = 0.502294
c       //// READING THE INPUT FILE ////
        do 20 k = 1, N
        read (8,*) tt
        sum1 = 0.
        sum2 = 0.
        tt = float(k)/100.0
        alnt = alog(tt)
c       //// CALCULATION OF SAMPLE RADIUS ////
        f = -alnt/amu/2.
        r = f
        do 10 i = 1,nmax
c       //// GENERATION OF RANDOM POINTS IN SAMPLE VOLUME ////
        a = aphasa (-f, f)
        b = aphasa (-f, f)
        c = aphasa (-f, f)
        abc = sqrt (a*a + b*b + c*c)
        if (abc.gt.f) goto 10
c       //// GENERATION OF RANDOM POINTS ON DETECTOR SURFACE ////
        c1 = aphasa (-dr, dr)
        pp = sqrt (dr*dr - c1*c1)
        a1 = aphasa (-pp, pp)
c       //// CALCULATION OF (X,Y,Z) ////
        p = (d-b)**2+(c1-c)**2+(a1-a)**2
```

```
      q = -2.0*((c1-c)*(b*c1-c*d)+(a1-a)*(b*a1-a*d))
      s = f**2*(d-b)**2
      s = -(s-(b*c1-c*d)**2-(b*a1-a*d)**2)
      y1 = q*q-4.0*p*s
      y = (-q + sqrt(y1))/(2.0*p)
      z = (x*(c1-c)-b*c1+c*d)/(d-b)
      x = (x*(a1-a)-b*a1+a*d)/(d-b)
c     //// CALCULATION OF NUMERATOR AND DENOMINATOR OF EQN 13 ////
      t = sqrt((b-y)**2+(c-z)**2+(a-x)**2)
      rsquare = ((b-d)**2+(c-c1)**2+(a-a1)**2)
      term = (exp(-amu*t))/rsquare
      sum1 = sum1+(1./rsquare)
      sum2 = sum2+term
10    continue
c     //// ATTENUATION CORRECTION FACTOR CALCULATION ////
      cfat = sum1/sum2
c     //// WRITING THE OUTPUT IN FILE ////
      write (9,*) tt, f, cfat
20    continue
      end
      function aphasa(x1, x2)
c     aphasa
c     random floating point number equally distributed between x1 and x2
      double precision a, b
      data a /.78149275363e0/
      b = (a+11d0/87d0)*87d0
      i = b
      a = b-i
      aphasa = x1+(x2-x1)*a
      return
      end
```

Program 4.

```
c ***********************************************************************
cc --- Attenuation correction factors for disc geometry -------
c ***********************************************************************
c         //// DESCRIPTION OF THE PARAMETERS ////
c         N = Number of input transmittance value for which attenuation
c         correction factor has to be calculated
c         f = Half - thickness of the disc
c         nmax = number of random points generated
c         d = sample to detector distance taken from the centre of the sample
c         amu = linear attenuation coefficient
c         tt = transmittance
c         r = radius of cylinder
c         dr = radius of detector crystal
c         CFAT = Attenuation correction factor
c         //// ALL THE QUANTITIES ARE IN CGS UNITS. ////
          N = 10
          nmax = 100000
c         //// OPENING AN INPUT AND OUTPUT FILE ////
          open(8, file='transm.txt')
          open(9, file='disc.out')
          d = 100.0
          r = 1.27
c         //// READING THE INPUT FILE ////
          do 20 k = 1,16
          read(8,*) tt
          tt = float(k)/100.0
          alnt = alog(tt)
c         //// CALCULATION OF SAMPLE THICKNESS ////
          f = -alnt/amu/2.
          sum1 = 0.
          sum2 = 0.
          do 10 i = 1,nmax
c         //// GENERATION OF RANDOM POINTS IN SAMPLE VOLUME ////
          a = aphasa (0.0, r)
          b = aphasa (-f, f)
          c= aphasa (0.0, r)
          bb=sqrt(a*a + c*c)
          if (bb.gt.r) goto 10
c         //// GENERATION OF RANDOM POINTS ON DETECTOR SURFACE ////
          a1 = aphasa (-dr, dr)
          c1 = aphasa (-dr, dr)
          aaa = sqrt(a1*a1 + c1*c1)
          bbb = dr
          if(aaa.gt.bbb) goto 10
```

```
      z = (f*(c1-c)-b*c1+c*d)/(d-b)
      x = (f*(a1-a)-b*a1+a*d)/(d-b)
      aa = sqrt(x*x + z*z)
      bb = r
      if(aa.gt.bb) then
c     //// CALCULATION OF (X,Y,Z) ////
      p = (c1-c)**2+(a1-a)**2
      q = 2.0*(a1-a)*(a*c1-a1*c)
      s = r**2*(c1-c)**2
      s = -(s-(a*c1-c*a1)**2)
      y = q*q-4.0*p*s
      y1 = (-q+sqrt(y))/(2.0*p)
      y2 = (-q-sqrt(y))/(2.0*p)
      z = (y1*(c1-c)-b*c1+c*d)/(d-b)
      x = (y1*(a1-a)-b*a1+a*d)/(d-b)
c     //// CALCULATION OF NUMERATOR AND DENOMINATOR OF EQN 13 ////
      t = sqrt((b-y1)**2+(c-z)**2+(a-x)**2)
      rsquare = ((b-d)**2+(c-c1)**2+(a-a1)**2)
      t = sqrt((b-f)**2+(c-z)**2+(a-x)**2)
      rsquare = ((b-d)**2+(c-c1)**2+(a-a1)**2)
      term = (exp(-amu*t))/rsquare
      sum1 = sum1 + (1./rsquare)
      sum2 = sum2 + term
10    continue
c     //// ATTENUATION CORRECTION FACTOR CALCULATION ////
      cfat = sum1/sum2
c     //// WRITING THE OUTPUT IN FILE ////
      write( 9,*) tt, cfat
20    continue
      end
      function aphasa(x1, x2)
c     aphasa
c     random floating point number equally distributed between x1 and x2
      double precision a, b
      data a /.78149275363e0/
      b = (a+11d0/87d0)*87d0
      i = b
      a = b-i
      aphasa = x1+(x2 - x1)*a
      return
      end
```